

# Renewable Resource based blends of Polylactic acid (PLA) and Thermoplastic starch (TPS) using Novel Reactive Compatibilization

SUKHILA KRISHNAN\*, SMITA MOHANTY AND SANJAY K.NAYAK

*Laboratory for Advanced Research in Polymeric Materials (LARPM), Central Institute of Plastic Engineering and Technology (CIPET), Bhubaneswar, INDIA*

## ABSTRACT

*The current work deals with enhancing the compatibility between thermoplastic starch (TPS) and polylactic acid (PLA) blends. TPS was initially modified with methylene diphenyldiisocyanate (MDI) / epoxidized soybean oil (ESO) to reduce its hydrophilic nature. The effect of MDI / ESO incorporation on the properties of PLA/TPS blend was evaluated by employing thermal, mechanical, morphological and water absorption studies. Morphological studies showed that in comparison to TPS, TPS modified by MDI and ESO were uniformly dispersed within the PLA matrix and exhibited higher impact energy as compared with neat PLA.*

**KEYWORDS:** *Polylactic acid (PLA), Thermoplastic starch (TPS), Methylene diphenyl diisocyanate (MDI), Epoxidized soybean oil (ESO), Compatibility.*

## 1. INTRODUCTION

Polylactic acid (PLA) has been the material of choice due to its high-strength, high-modulus and biodegradable nature. PLA is an ecofriendly polymer and has potential strength to substitute petroleum based products for manifold applications. However, PLA shows a lot of limitations such as low flexibility, elongation at break, toughness and limited processability which hinders its use in niche

applications. PLA is expensive as compared with other conventional petroleum based polymers. Hence, in order to reduce the cost of processing materials, starch is the best option as it is a renewable raw material, biodegradable, abundantly available and inexpensive. Many studies have been carried out in the area of PLA/starch blends to reduce the production cost and improve its biodegradability<sup>[1]</sup>. Furthermore, to enable the

---

J. Polym. Mater. Vol. 34, No. 3, 2017, 525-538

© Prints Publications Pvt. Ltd.

Correspondence author e-mail: sukhilaaajith@gmail.com

melt mixing of starch with polymer, it has been suitably thermoplasticized to Thermoplastic starch (TPS), as pure starch has a melting temperature of around 220-240°C, which is close to its degradation temperature [2-4]. Commonly employed plasticizers for modification of starch includes polyols such as sorbitol and glycerol as they are generally similar to the structure of the polymer they plasticize [5]. Therefore, to enhance the interfacial adhesion between PLA and TPS, the reactive compatibilizer such as maleic anhydride, methylenediphenyl diisocyanate (MDI) or plasticizers like ESO were intended to initiate chemical bonds between PLA and TPS molecules [6-19]. Further, substitution of isocyanate groups has seemed much consideration as compatibilizers in PLA and starch blends. Especially, MDI has been extensively studied and several workers have reported improved mechanical properties in the PLA/starch blends. Yu et al had investigated PLA/starch blends with and without MDI and had reported the effects of MDI incorporation and its distribution on the various properties of blends [11]. Another work, with MDI as an coupling agent for PLA/starch blends was reported by Wang et al [16]. ESO due to its non toxic has been utilized to decrease water absorption and to enhance the service life of concrete. Tee et al had noted that both the epoxidized palm oil and ESO can act as an effective plasticiser for PLA [20]. ESO also acts as a plasticizer in many polymeric systems, which is predominantly due to the presence of polar groups that enhances the mechanical properties, essential for improved compatibility. Ali et al had analyzed the plasticization effect of ESO in lowering the modulus, viscosity and glass transition

temperature while improving the elongation at break of the PLA/ESO blends [21].

In this study, a novel approach for improving the compatibility between starch and PLA is considered via modification of starch using MDI and ESO. Further, the blend of PLA with TPS has been prepared employing melt blending technique. A comparative aspect of the properties of PLA blends with TPS and modified TPS; using MDI as well as ESO has been investigated. An in depth analysis of mechanical, thermal, morphological and water absorption characteristics of PLA and its blends has been studied.

## 2. EXPERIMENTAL

### 2.1 Materials

PLA (4042 D) was obtained from M/s Nature Works LLC, USA. Tapioca starch was procured from M/s Angel Starch and Food Pvt Ltd, Erode, India. Other chemicals like Glycerol (AR), Triethylamine were purchased from M/s Merck specialities Pvt Ltd. Mumbai, India, Dibutyltindilaurate (DBTDL) and 4,4'-methylenebis(phenyl isocyanate) (MDI) was procured from M/s Sigma Aldrich, Hyderabad, India. The chemical pure grade of epoxidized soybean oil having an epoxy equivalent of 0.46 was purchased from M/s Chempure Mumbai, India.

### 2.2 Preparation of Thermoplastic Starch (TPS)

Prior to use, tapioca starch was dried in a vacuum oven at 70°C for 4hr. The pre-mix was allowed to mix aggressively in a batch mixer (M/s Haake Rheomix 600, Germany) at a temperature of 130°C and rotor speed of 50 rpm for 6 min. The composition of TPS reported in the current study is 5wt % water, 25 wt % glycerol and 70 wt % starch.

Modification of TPS has been carried out using MDI and ESO. The dried TPS (100g) was mixed aggressively in a batch mixer with MDI (3,5,7 wt%) and DBTDL (0.05g) at a temperature of 130°C and rotor speed of 50 rpm for 6 min. The chemical structures of modified TPS were

confirmed by FTIR and <sup>1</sup>H NMR as discussed in subsequent sections. MDI modified TPS is termed as M-TPS in further discussion.

The dried TPS samples (100g) and ESO (1,3,5 wt%) were mixed aggressively in a batch mixer with catalyst triethylamine (TEA) which facilitates the condensation reaction between the hydroxyl group of TPS and epoxide rings of ESO at a temperature of 130°C and rotor speed of 50 rpm for 6 min. The modified TPS was dried in oven at 60-80°C and kept in a desiccator for further characterization. The ESO grafted TPS was confirmed using FTIR analyser and <sup>1</sup>H NMR spectra. ESO modified TPS is termed as E-TPS in further discussion.

### 2.3.3 Preparation of PLA/TPS Blends

The PLA/TPS, PLA/M-TPS and PLA/E-TPS blends at variable compositions were prepared in a batch mixer (Haake Rheomix 600, Germany) at a temperature of 165°C and the speed of 50 rpm for a mixing time of 6 min. Further, specimens were prepared using micro injection jet (DSM 15mL xplora, Netherlands). The molding was carried out at a process temperature of 155°C with a screw speed of 60 rpm. The mould temperature was kept at 35°C and molding was carried out at an injection pressure of 145 psi. The PLA/TPS blend composition was optimized based on mechanical properties, which was subsequently used to prepare PLA blends with modified TPS. The formulations based on the compositions of each blend is represented in table 1.

TABLE 1. The sample codes and compositions

| Sample code                          | TPS (wt %) | MDI (wt %) | ESO (wt %) | PLA (wt %) |
|--------------------------------------|------------|------------|------------|------------|
| PLA/TPS <sub>1</sub>                 | 20         | 0          | 0          | 80         |
| PLA/TPS <sub>2</sub>                 | 25         | 0          | 0          | 75         |
| PLA/TPS <sub>3</sub>                 | 35         | 0          | 0          | 65         |
| PLA/TPS <sub>4</sub>                 | 45         | 0          | 0          | 55         |
| PLA/M <sub>3</sub> -TPS <sub>1</sub> | 20         | 3          | 0          | 80         |
| PLA/M <sub>5</sub> -TPS <sub>1</sub> | 20         | 5          | 0          | 80         |
| PLA/M <sub>7</sub> -TPS <sub>1</sub> | 20         | 7          | 0          | 80         |
| PLA/E <sub>1</sub> -TPS <sub>1</sub> | 20         | 0          | 1          | 80         |
| PLA/E <sub>3</sub> -TPS <sub>1</sub> | 20         | 0          | 3          | 80         |
| PLA/E <sub>5</sub> -TPS <sub>1</sub> | 20         | 0          | 5          | 80         |

### 3. Characterization

FTIR analysis of the modified and unmodified TPS samples (about 4mg) was performed using ThermoNicolet 6700 FTIR spectrometer, Thermofisher, USA. The <sup>1</sup>H NMR spectra was performed on a 400MHz Bruker AVANCE III nuclear magnetic resonance (NMR) spectrometer Bruker, Switzerland, with DMSO as a solvent.

Universal Testing Machine (M/s Instron 3382, UK) was employed to determine the tensile strength, tensile

modulus and elongation at break (EB). Dumb-bell shaped specimens prepared from PLA and its blends having dimensions of 165×12.7×3mm were tested at a crosshead speed of 5mm/min with a gauge length of 100 mm along with a load cell of 10 KN as per ASTM D 638. The notched impact strength of PLA and its blends samples having the dimensions of 63.5×12.7×3mm was performed according to ASTM D 256 in an impact tester (M/s Tinius Olsen, USA).

Differential scanning calorimetry (DSC Q20, M/s TA instruments, USA) was used to analyze the thermal

transitions i.e. glass transition temperature ( $T_g$ ), crystallization temperature ( $T_c$ ) and melting temperature ( $T_m$ ) of PLA and its blends. Samples (5-10mg) were heated from temperature -50 to 250°C at a heating rate of 20°C/min for a first heating scan, then the samples were cooled to -50°C at a cooling rate of 20°C/min, held at -50°C for 5 min, and then again heated from -50 to 250°C at a heating rate of 20°C/min in an  $N_2$  atmosphere.

In accordance to ASTM D 570-81 standard, moisture absorption of PLA and its blends were calculated. The samples were fully immersed in distilled water (25°C) and at regular intervals taken out of the water. Then, excess water on the surface was wiped with tissue paper, weighed and again reimmersed in distilled water. Water absorption ( $M_t$ ) was calculated by the formula:

$$M_t(\%) = \frac{W_t - W_0}{W_0} \times 100\%$$

Where  $W_0$  and  $W_t$  are the weights of the sample before and after moisture absorption at time  $t$  respectively.

Based on the absorption curves linear interrelation, the diffusion coefficient ( $D$ ) can be determined by the equation based on Fick's law

$$\frac{M_t}{M_\infty} = (4/\pi^{1/2}) (1/b)(Dt)^{1/2}$$

Where  $M_t$  and  $M_\infty$ , respectively, is the quantity of the water absorbed at time  $t$  and at equilibrium absorption time,  $b$  is the thickness of the sample,  $D$  is the diffusion coefficient and  $t$  is time. [22]

Water permeability of PLA blends depends on diffusion coefficient as well as sorption coefficient of water in the sample. Sorption coefficient  $S$  can be expressed by the formula. [23,24]

$$S = \frac{W_\infty}{W_0}$$

$W_0$  and  $W_\infty$ , respectively, is the initial weight of sample taken before water absorption and after absorption reaching the equilibrium. The permeability coefficient ( $P$ ) of the blends can be calculated by the following formula. [23,24]

$$P = D \times S$$

The morphology of the prepared blends was analyzed using scanning electron microscopy (SEM) EVO MA 15 (M/s Carl Zeiss, SMT Ltd, Germany) at an accelerated voltage of 5KV. Cryofractured sample was used for the analysis and the test surface was gold coated prior to the testing.

## 4. RESULTS AND DISCUSSION

### 4.1 FTIR Analysis of modified TPS, PLA and its blends

The FTIR absorption spectra of starch, TPS, M-TPS, E-TPS are shown in the Fig. 1. The raw starch spectrum shows characteristic O-H stretching peak at 3286  $cm^{-1}$ , C-H stretching peak at 2928  $cm^{-1}$ , C-O peaks 1000-1150  $cm^{-1}$  and other peaks due to bending stretches. The spectrum of TPS displays two new absorption peaks at 2867  $cm^{-1}$  and 1105  $cm^{-1}$  which corresponds to the C-H stretching and C-O stretching respectively. Within the TPS polymer chains, the plasticizer is embedded, causing distortion in the basic starch structure, thereby shifting the wavenumber of the C-H bending peak marginally [25]. FTIR pattern of E-TPS exhibited a new peak at 1743  $cm^{-1}$  which attributes to - C=O stretching of the triglyceride's ester group. As the content of ESO is very less, no other peaks relevant to the structure of ESO was detected in the FTIR spectra. The presence of C-O-C stretching peak at 1743  $cm^{-1}$  shows a possible condensation reaction between hydroxyl groups (present in both starch and glycerol) and the epoxide ring of ESO, as the reaction proceeds [26]. FTIR spectra of M-TPS shows C-O and C=O stretching vibration peak of the urethane at 1725  $cm^{-1}$  and 1644  $cm^{-1}$  respectively, and the shoulder peak at 1704  $cm^{-1}$  attributes to H-bonded urethane groups. Due to C-N and C-O

stretching of urethane, the peak at  $1534\text{ cm}^{-1}$  and  $1225\text{ cm}^{-1}$  appeared as doublet, confirming isocyanate groups of MDI forms urethane linkage with the hydroxyl groups of TPS [27].

Additionally, the isocyanate peak at  $2281\text{ cm}^{-1}$  was also observed. Hence, the successful modification of TPS using ESO and MDI was confirmed from the FTIR analysis.

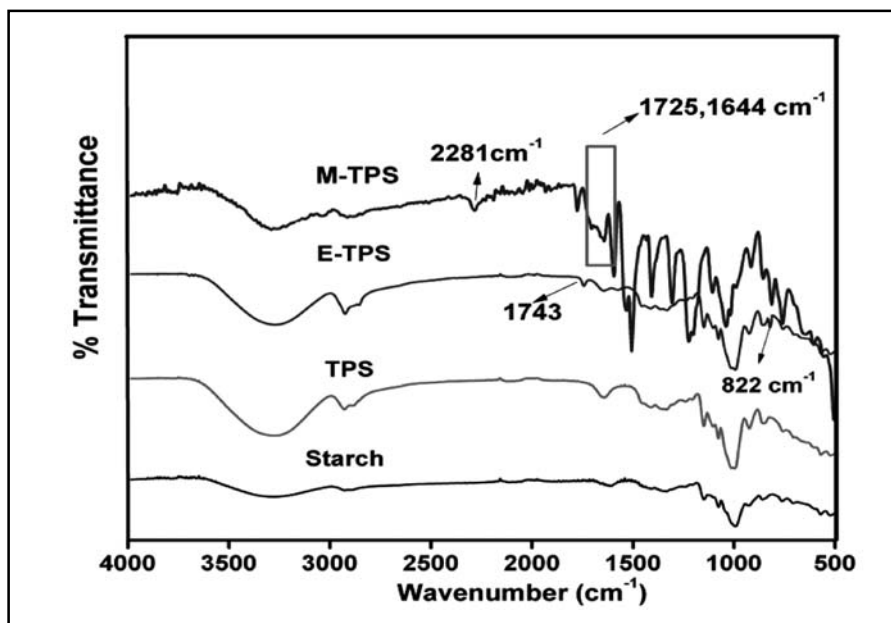


Fig. 1. The FTIR spectra of M-TPS and E-TPS

#### 4.2 $^1\text{H}$ NMR spectroscopy of modified TPS

As shown in the spectrum (Fig. 2), the signals due to the  $-\text{OH}$  groups of TPS appeared in the region 3.5-5.8 ppm. The peaks with respect to hexamethylene group were visible in the region 3.78 ppm. The peak in the region 7-7.35 ppm represents the proton of aromatic structure and the signal at 8.74 ppm shows the presence of urethane linkage in M-TPS sample [28]. Three distinct signals were observed in between 2.85-3.25 ppm for the oxirane ring hydrogen of linolenic acid of ESO. The glyceride structure in the ESO shows an NMR signal at 4.0-4.4 ppm and 5.1 ppm [29].

#### 4.3 Mechanical Properties of PLA and its blends

The mechanical properties (impact and tensile) of virgin PLA and its blends were analyzed and the results are summarized in Table 2. Analysis revealed that blending of PLA with TPS results in a decrease in the mechanical properties. Tensile modulus of PLA exhibited a decrease to the tune of 5.6%, 10.4%, 11.1% and 30% with a TPS content of 20%, 25%, 35% and 45%. This observation was in accordance with the findings reported by Muller et al [30], wherein the author observed that the addition of TPS within PLA exhibits decreased modulus. The

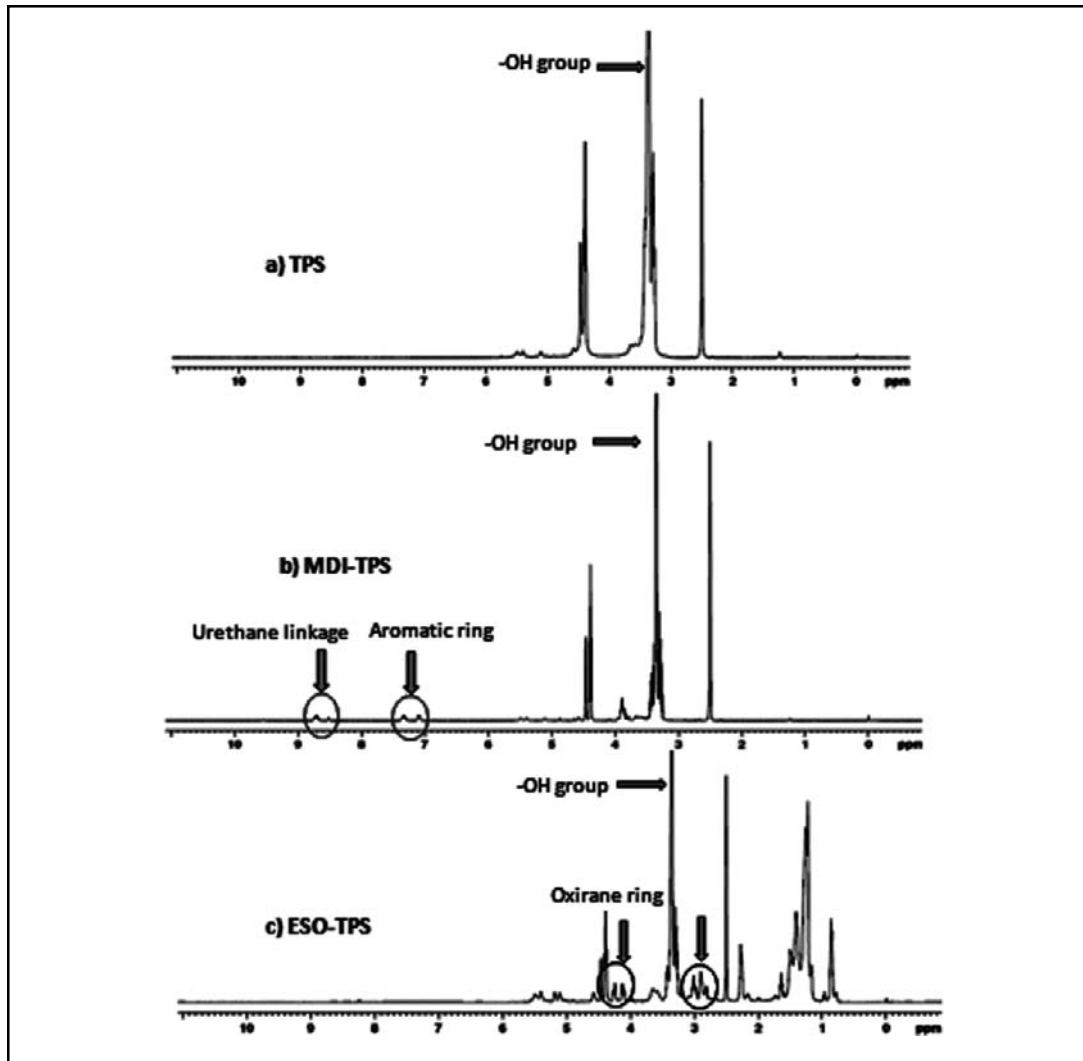


Fig. 2  $^1\text{H}$  NMR spectra of TPS, MDI-TPS and ESO-TPS.

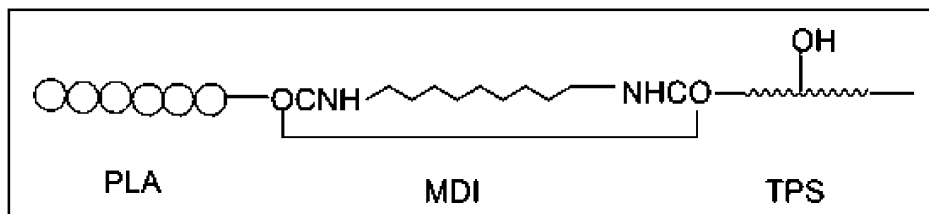
lowered tensile strength of PLA after incorporation of TPS, suggested lack of compatibility between hydrophilic TPS and hydrophobic PLA that in turn leads to the poor distribution of stress at the interface during application of external loads <sup>[13]</sup>. As, the plasticizer content (glycerol) increases, the

modulus and tensile strength decreases <sup>[2,16]</sup>. Based on the maximum tensile modulus, blend composition PLA/TPS<sub>1</sub> (80:20) was considered as optimum and used for further investigation. The lower elongation at break (EB) of the PLA with the incorporation of TPS at various loading of TPS revealed the discontinuity of the matrix

polymer with an increase in the TPS as dispersed phase. This result was in accordance with the findings reported by Ohkita et al [22].

To improve the compatibility between PLA and TPS, TPS was modified using MDI and ESO prior to blending with PLA. As observed from the table, increase in MDI concentration from 3 to 5 wt % resulted in increased tensile strength and modulus of PLA in the PLA/M-TPS blends. An increase of 8% in impact strength and 19% in tensile modulus was obtained in case of PLA/M<sub>5</sub>-TPS<sub>1</sub> blend as compared with virgin PLA. This behaviour is due to improved compatibility between PLA and TPS. However, at 7wt% of MDI, the mechanical properties shows deterioration which may be reasonably due to the consumption of excess MDI by water/glycerol absorbed in TPS, that leads to weakening of coupling bond in between the TPS and PLA phases [11]. Test results

reported in table also revealed that the impact strength of the PLA/M<sub>5</sub>-TPS<sub>1</sub> blend was higher to the tune of 69 % as compared with PLA/TPS<sub>1</sub>. This reveals improved compatibility between TPS and PLA via modification of TPS using MDI wherein, the later acts as a bridge between PLA and TPS. Furthermore, it is also assumed that during mixing isocyanate group in MDI interacts with free hydroxyl groups of PLA and TPS resulting in the formation of graft copolymer of PLA and TPS, while increasing the crosslinking between both the phases. The interactions between PLA-MDI-TPS were confirmed by FTIR analysis as represented in Scheme 1. The tensile modulus of PLA/M<sub>5</sub>-TPS<sub>1</sub> was also higher as compared with PLA and PLA blends with unmodified TPS, confirming similar facts of improved stress transfer at the interface with the addition of MDI [22]. Furthermore, no appreciable improvement in tensile strength of PLA/M<sub>3</sub>-TPS<sub>1</sub> could be noticed as compared with that of PLA/TPS<sub>1</sub>.



Scheme 1. Possible interaction site of PLA with TPS in presence of MDI through reactive processing.

The mechanical properties of PLA/E-TPS<sub>1</sub> blends with different wt% of ESO (1-5wt%) is also depicted in table 2. It was observed that, PLA blend with ESO modified TPS (E<sub>3</sub>-TPS<sub>1</sub>) exhibited higher impact strength, elongation at break and tensile modulus as compared with virgin PLA, PLA/TPS<sub>1</sub> and PLA/M<sub>5</sub>-TPS<sub>1</sub>, respectively. This behaviour revealed improved toughness of the PLA after incorporation of

ESO modified TPS and efficient compatibilizing effect of ESO onto the PLA and TPS. This is attributed to the fact that ESO covers the TPS molecules, providing a plasticizing effect as well as active sites to the free hydroxyl group of PLA, resulting in the crosslinking interaction between them. Above 3 wt% of ESO, the tensile modulus and impact strength decreased. This may be

TABLE 2. Mechanical properties of PLA and its blends

| Sample                               | Impact strength (J/m) | Tensile strength (MPa) | Elongation at break (%) | Tensile Modulus (MPa) |
|--------------------------------------|-----------------------|------------------------|-------------------------|-----------------------|
| Virgin PLA                           | 25±2                  | 56±3                   | 2.3±0.1                 | 1958 ± 20             |
| PLA/TPS <sub>1</sub>                 | 16 ± 2                | 35±1                   | 1.57±0.1                | 1847 ± 70             |
| PLA/TPS <sub>2</sub>                 | 14 ± 1                | 32 ± 8                 | 2 ± 0.15                | 1754 ± 53             |
| PLA/TPS <sub>3</sub>                 | 14.3±1                | 24 ± 4                 | 1.2 ± 0                 | 1740 ± 1              |
| PLA/TPS <sub>4</sub>                 | 14±0.5                | 28 ± 5                 | 1.6±0                   | 1367 ± 11             |
| PLA/M <sub>3</sub> -TPS <sub>1</sub> | 20±1.2                | 32±0.5                 | 1.4±0.2                 | 1935±14               |
| PLA/M <sub>5</sub> -TPS <sub>1</sub> | 27±1                  | 33±0                   | 1.7±0                   | 2441 ± 24             |
| PLA/M <sub>7</sub> -TPS <sub>1</sub> | 24±1.6                | 30±2                   | 1.5±0.1                 | 2366±16               |
| PLA/E <sub>1</sub> -TPS <sub>2</sub> | 25±0.5                | 31±1                   | 2.1±0.15                | 2543±40               |
| PLA/E <sub>3</sub> -TPS <sub>1</sub> | 30±2                  | 34±10                  | 4.5±0.1                 | 2860 ± 83             |
| PLA/E <sub>5</sub> -TPS <sub>1</sub> | 28±2.3                | 32±3                   | 4.0±0                   | 2500±33               |

examined as the critical interfacial concentration at which saturation is attained for ESO in the interphase. Therefore, it may be concluded that ESO acts as an interconnecting media between PLA and TPS, hence provides compatibilization effect within the blend [18,31]. Additionally, the mechanical properties of PLA/E<sub>3</sub>-TPS<sub>1</sub> was found to be higher than that of PLA/M<sub>5</sub>-TPS<sub>1</sub> with impact strength of Virgin PLA increasing from 25 J/m to 30J/m. This reveals the relatively higher compatibility of PLA with E-TPS as compared with M-TPS which is due to the fact that some of the MDI forms urea in the presence of water. The schematic representation of interactions in PLA/E-TPS<sub>1</sub> and PLA/M-TPS<sub>1</sub> is given in Scheme 2.

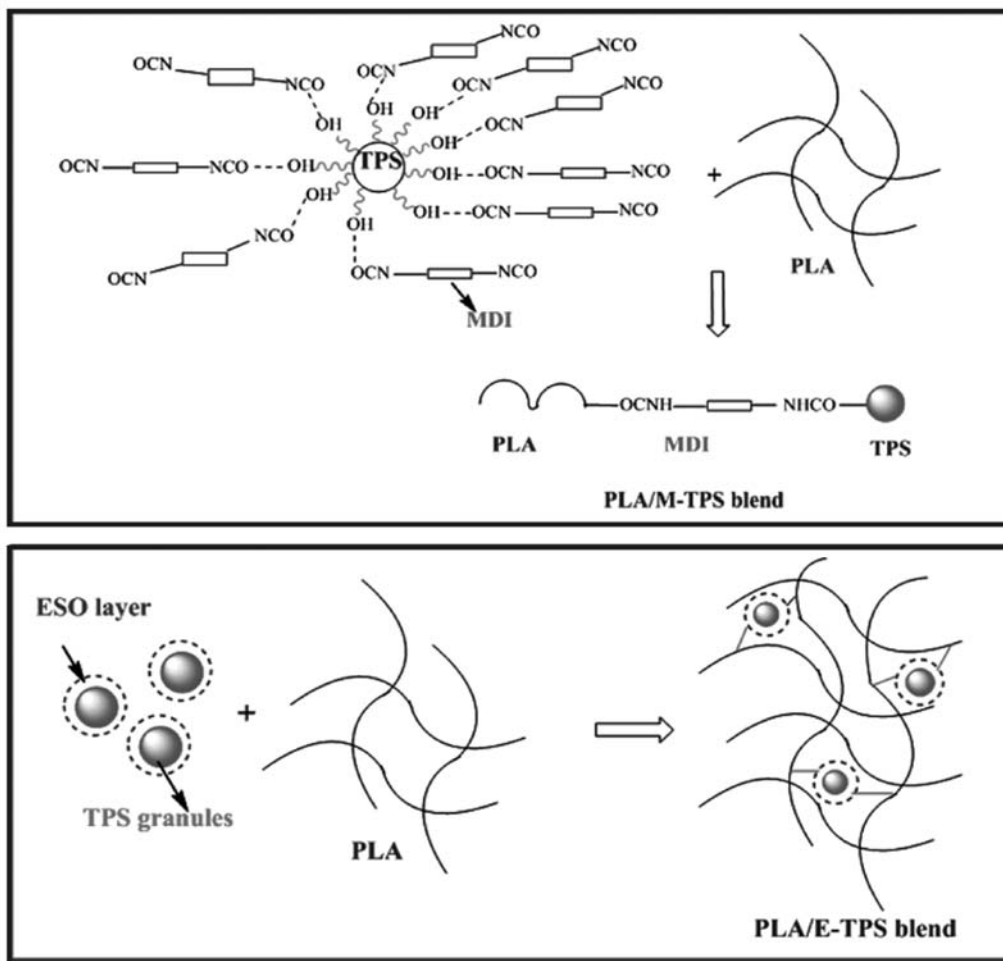
#### 4.4 Thermal Properties of PLA and its blends

Thermal properties of virgin PLA and its blends were observed employing DSC analysis and

the values are summarized in Fig. 3 and Table 3. DSC thermograms from the second heating cycle revealed the  $T_g$ ,  $T_m$  and crystallinity of the PLA blends. The melt temperature of blends, show trivial variation in comparison to virgin PLA. The virgin PLA shows a  $T_g$  at 59.2°C and the addition of TPS within the matrix polymer leads to decrease in the  $T_g$  of PLA to 54.4°C. However, the shifts become prominent in the presence of MDI and ESO with  $T_g$  values at 51°C and 49°C respectively. At the same time, the cold crystallization temperature of PLA and its blends reduced, with  $T_{cc}$  for PLA, PLA/TPS<sub>1</sub>, PLA/M<sub>5</sub>-TPS<sub>1</sub>, PLA/E<sub>3</sub>-TPS<sub>1</sub> at 128°C, 103°C, 99°C and 96°C respectively, which is attributed to enhanced mobility of PLA in presence of plasticizer that facilitates the  $T_{cc}$  of PLA at lower temperature.

In case of PLA/M<sub>5</sub>-TPS<sub>1</sub>, low  $T_{cc}$  (99°C) is mainly due to the functional group isocyanate that reacted with PLA chains to undergo





Scheme 2. The schematic reaction of PLA and modified starch blends  
(a) PLA and MDI modified TPS blends (b) PLA and ESO modified TPS blends.

hydrogen bond reaction forming  $\text{-NH-CO-}$  groups<sup>[32,33]</sup> while in case of  $\text{PLA/E}_3\text{-TPS}_1$ ,  $T_{cc}$  at  $96^\circ\text{C}$  is directly linked to increased chain mobility attributed to the internal lubrication effect that ESO causes, which is similar to the study of Z. Xiong et al.<sup>[20]</sup> and Ali et al.<sup>[21]</sup>. The depression of  $T_{cc}$  and lowering of  $T_g$  reveals that the MDI and ESO were compatible with PLA<sup>[16]</sup>

TABLE 3. DSC studies showing glass transition temperature ( $T_g$ ), cold crystallization temperature ( $T_{cc}$ ), melting temperature ( $T_m$ ) of PLA and its blends

| Sample                        | $T_g$ ( $^\circ\text{C}$ ) | $T_m$ ( $^\circ\text{C}$ ) | $T_{cc}$ ( $^\circ\text{C}$ ) |
|-------------------------------|----------------------------|----------------------------|-------------------------------|
| PLA                           | 59.2                       | 157                        | 128                           |
| $\text{PLA/TPS}_1$            | 54.4                       | 155                        | 103                           |
| $\text{PLA/M}_5\text{-TPS}_1$ | 51                         | 158                        | 99                            |
| $\text{PLA/E}_3\text{-TPS}_1$ | 49                         | 158                        | 96                            |

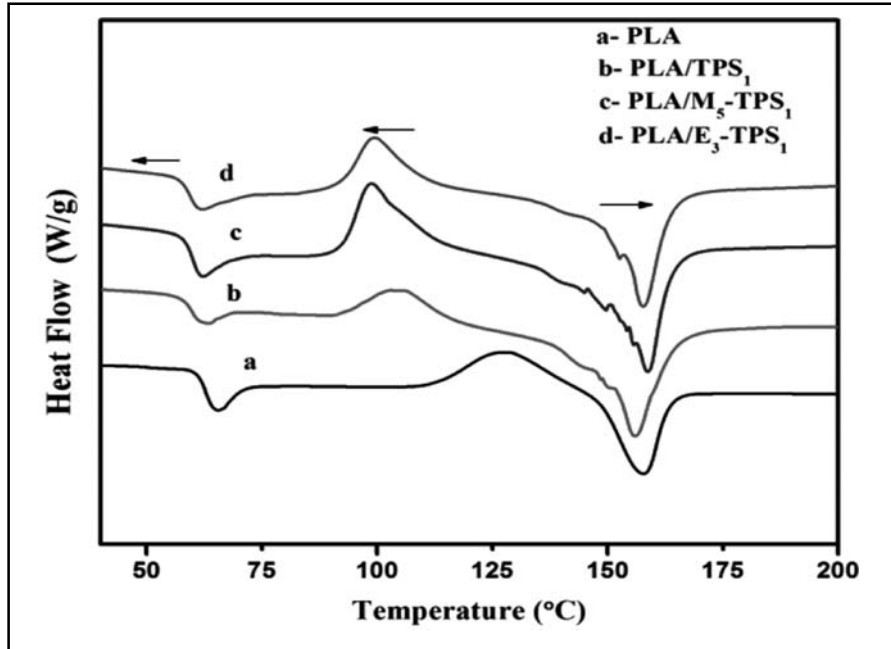


Fig. 3. DSC thermograms of virgin PLA and its blends

#### 4.5 Water Absorption Behaviour of PLA and its blends

The effect of MDI and ESO on the water absorption behavior of the PLA blends was evaluated and the results are summarized in Fig. 4 and Table 4. As one of the main limitations in the use of starch based blends is their hydrophilic nature, so any improvement towards hydrophobic nature is of vital importance<sup>[34]</sup>. Water absorption is related to its rate of diffusion into blends. The graph represents a relation between absorbed water (%) vs ratio of the square root of time and the thickness of the specimen. PLA showed a linear curve nearly horizontal to X-axis, indicating the negligible amount of water absorption ( $M_t$ ). In all the cases of blends, initially a linear increase in the  $M_t$  was noticed revealing the absorption of water

due to the presence of hydrophilic starch content. Further, after a certain point, the  $M_t$  exhibited a constant value and no further increase in the  $M_t$  was obtained.

The point at which the  $M_t$  becomes constant, exhibits the saturation point for water absorption indicating Fickian behaviour in the blends. From the figure, it is evident that the saturation point for PLA blend with  $M_5$ -TPS<sub>1</sub> and  $E_3$ -TPS<sub>1</sub> shifted towards the longer time period, indicating the delayed and slow water absorption rate as compared with PLA/TPS<sub>1</sub> blends. Furthermore, it is also observed that over the entire test duration  $M_t$  for PLA blends with modified TPS were lower as compared with PLA/TPS<sub>1</sub> blends. The order of  $M_t$  over the entire time duration is minimum for PLA/ $E_3$ -TPS<sub>1</sub> blends, in comparison to PLA/TPS<sub>1</sub> blends.

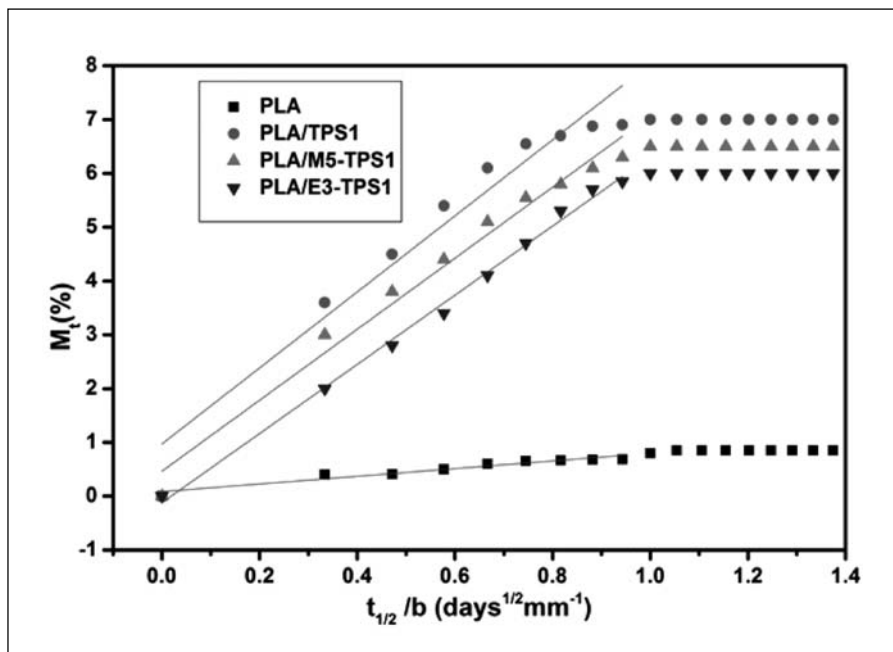


Fig. 4. Water absorption behavior of PLA and its blends

TABLE 4. PLA and its blends regression square ( $R^2$ ), sorption coefficient (S), diffusion coefficient (D) and permeability coefficient (P) at room temperature.

| Sample                               | $R^2$  | $D \times 10^{-6} (\text{mm}^2 \text{s}^{-1})$ | $S (\text{gg}^{-1})$ | $P \times 10^{-6} (\text{mm}^2 \text{s}^{-1})$ |
|--------------------------------------|--------|--|----------------------|--|
| PLA                                  | 0.9309 | 1.99   | 0.883                | 1.76   |
| PLA/TPS <sub>1</sub>                 | 0.9161 | 4.06   | 1.074                | 4.36   |
| PLA/M <sub>5</sub> -TPS <sub>1</sub> | 0.9762 | 3.12   | 0.967                | 3.01   |
| PLA/E <sub>3</sub> -TPS <sub>1</sub> | 0.9951 | 2.19   | 0.903                | 1.98   |

PLA/TPS<sub>1</sub> blends exhibited higher diffusion, sorption and permeability as compared to virgin PLA [35,36]. In comparison to PLA/TPS<sub>1</sub>, diffusion coefficients were less for blends with MDI or ESO, showing that the water diffusion into blends in presence of MDI or ESO proceeds slowly, with minimum diffusion for PLA/E<sub>3</sub>-TPS<sub>1</sub> blends. This may be due to the increased interfacial adhesion between PLA matrix and

TPS in the presence of MDI or ESO, which restricts the diffusion of water within the blends.

#### 4.6 Scanning electron microscopy (SEM) analysis of PLA and its blends

The fractured surfaces of the virgin PLA, PLA/TPS<sub>1</sub>, PLA/M<sub>5</sub>-TPS<sub>1</sub> and PLA/E<sub>3</sub>-TPS<sub>1</sub> blends were examined by SEM in Fig.5. In comparison to the smooth fractured surface of virgin PLA,

the PLA/TPS<sub>1</sub> blends exhibited gaps between PLA matrix and the plasticized starch, where the surface of the sample was rough. Additionally, many starch granules were not completely plasticized and few of them were separated from the surface of the sample causing cavities in the fracture surface, because of high interfacial tension and less interfacial adhesion between hydrophilic starch and hydrophobic PLA. This resulted in a decreased flexibility and orientation of starch while processing [37].

Meanwhile, in the presence of isocyanate, [22] TPS was uniformly dispersed in the PLA matrix as interaction within the hydroxyl groups of TPS and PLA with isocyanate proceeds while processing at high temperature and shear. Without MDI, there arises many holes, through

which starch molecules were drawn out, and the gap was evident from fig 5(b). However, in presence of MDI, interfacial adhesion was enhanced as the surface was smooth devoid of gaps between PLA and TPS which is similar to the findings reported by Yu et.al [11]. Similarly, in case of PLA/TPS blend, the dispersion between TPS and PLA phases increased and a homogeneous system was noticed. This behaviour is primarily due to the presence of ESO, which readily penetrates into starch granules and during processing enhances the flexibility of starch. Also, ESO contributes in creation of cavities that induces deformation, wherein an extensive amount of energy can be absorbed, leading to high toughness [38]. The SEM micrographs can be well correlated with the improvement in impact strength in the PLA/M<sub>5</sub>-TPS<sub>1</sub> and PLA/E<sub>3</sub>-TPS<sub>1</sub> samples.

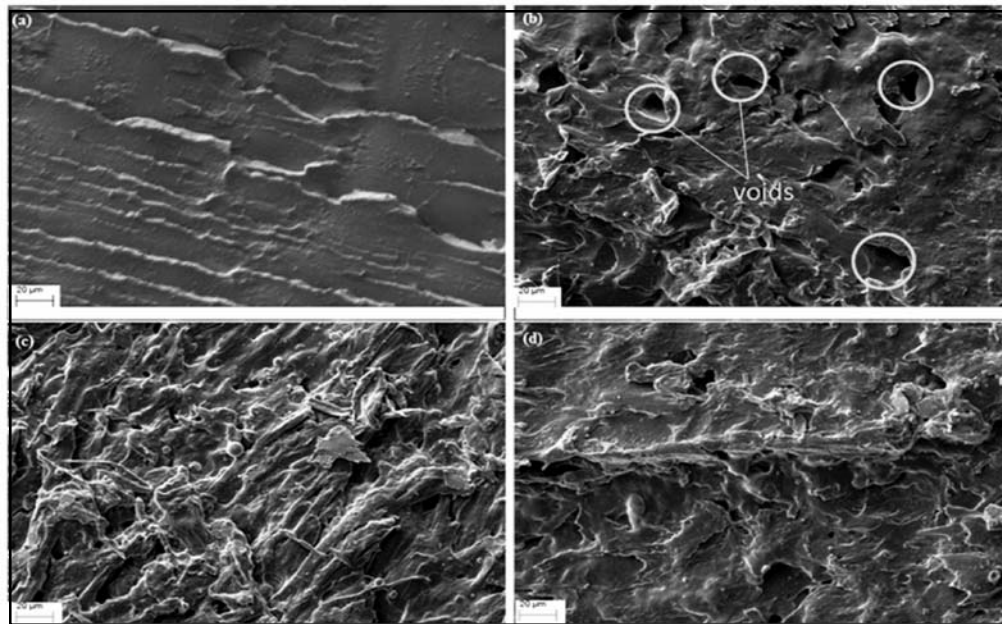


Fig. 5. SEM images of fractured surfaces of (a) Virgin PLA, (b) PLA/TPS<sub>1</sub> (c) PLA/M<sub>5</sub>-TPS<sub>1</sub> (d) PLA/E<sub>3</sub>-TPS<sub>1</sub>

## 5. CONCLUSIONS

In the current study, Thermoplastic Starch (TPS) was modified using MDI and ESO, for improving the interfacial adhesion with PLA. Modification of TPS with MDI or ESO, is a simple and cost effective method to tailor PLA/TPS blends with good mechanical and water resistant properties. ESO acts as a bio-based plasticizer and MDI as a compatibilizer which have effectively improved the mechanical, thermal and morphological properties of PLA and TPS blends. The results show that a small quantity of MDI or ESO forms a chemical bond with PLA and TPS which improves the interfacial adhesion as shown in SEM images. This is in agreement with the increment of mechanical properties. Hence, the findings reveal that modification of TPS with optimum quantity of MDI or ESO reduces the hydrophilic nature of PLA/TPS blends.

## ACKNOWLEDGEMENT

The authors acknowledge the Department of Chemicals and Petrochemicals, Ministry of Chemicals and Fertilizers, Govt. of India for financial support.

## REFERENCES

1. Krishnan, S., Pandey, P., Mohanty, S., Nayak, S. K. *Polym. Plast. Technol. Eng.* 2015, 55,1623-1652.
2. Sarazin, P., Li, G., Orts, W. J., Favis, B. D. *Polymer*. 2008, 49,599–609.
3. Souza, R., *Adv. Polym. Tech.* 2002, 21,17–24.
4. Stepto, R. *Macromol. Symp.* 2003, 201,201–212.
5. Gontard, N., Guilbert, S., CUQ, J. L. *J. Food Sci.* 1993, 58,206-211.
6. Zhang, J. F., Sun, X. Z. *Biomacromolecules*. 2004, 5, 1446–1451.
7. Wu, C. S. *Macromolecular Bioscience*. 2005, 5, 352–36.
8. Wang, H., Sun, X. Z., Seib, P. *J. Polym. Environ.* 2002,10, 133–138.
9. Teixeira, E. D. M., Curvelo, A. A., Correa, A. C., Marconcini, J. M., Glenn, G. M., Mattoso, L. H. *Ind. Crops Prod.* 2012, 37, 61-68.
10. Ren, J., Fu, H., Ren, T., Yuan, W. *Carbohydr. polym.* 2009, 77, 576-582.
11. Yu, L., Petinakis, E., Dean, K., Liu, H., Yuan, Q. *J. Appl. Polym. Sci.* 2011, 119, 2189–2195.
12. Tachaphiboonsap, S., Jarukumjorn, K. *Adv. Mat. Res.* 2013, 747, 67-71.
13. Yokesahachart, C., Yoksan, R. *Carbohydr. Polym.* 2011,83, 22–31.
14. Schwach, E., Six, J. L., Averous, L. *J. Polym. Environ.* 2008, 16, 286-297.
15. Shin, B.Y., Jang, S.H., Kim, B. S. *Polym. Eng. Sci.* 2011, 51,826–834.
16. Wang, H., Sun, X., Seib, P. *Journal of Applied Polymer Science*, 2001 82(7), 1761-1767.
17. Botaro, V. R., Gandini, A. *Cellulose*. 1998, 5, 65–78.
18. Carvalho, A.J.F., Curvelo, A.A.S., Gandini, *Ind. Crop. Prod.* 2005, 21,331–336.
19. Ferri, J. M., Garcia-Garcia, D., Sánchez-Nacher, L., Fenollar, O., Balart, R. *Carbohydr. Polym.* 2016, 147,60-68.
20. Tee, Y. B., Talib, R. A., Abdan, K., Chin, N. L., Basha, R. K., Yunos, K. F. M. *BioResources*, 2015, 11, 1518-1540.
21. Ali, F., Chang, Y. W., Kang, S. C., Yoon, J. Y. *Polym. Bull.* 2009, 62, 91-98.
22. Ohkita, T., Lee, S. H. *J.adhes. sci. Technol.*, 2004, 18, 905-924.

23. Sreekumar, P.A., Thomas, S.P., Saiter, J.M., Joseph, K., Unnikrishnan, G., Thomas, S. *Compos. Part A: Applied S.* 2009, 40, 1777–1784.
24. Sreekala, M.S., Thomas, S. *Compos. Sci. Technol.* 2003, 63, 861–869.
25. Musa, M. B., Yoo, M. J., Kang, T.J., Kolawole, E. G., Ishiaku, U. S., Yakubu, M. K., Whang, D. J. *J. Eng. Technol.* 2013, 2, 9-16.
26. Belhassen, R., Vilaseca, F., Mutjé, P., Boufi, S. *Ind. Crops Prod.* 2014, 53, 261-267.
27. Xiong, Z., Zhang, L., Ma, S., Yang, Y., Zhang, C., Tang, Z., Zhu, J. *Carbohydr. Polym.* 2013, 94, 235-243.
28. Yeganeh, H., Hojati-Talemi, P. *Polym. Degrad. Stab.* 2007, 92, 480-489.
29. Shah, D. U. *Scitech. J.* 2004, 1, 13-29.
30. Muller, C. M., Pires, A. T., Yamashita, F. *J. Brazil. Chem. Soc.* 2012, 23, 426-434.
31. Robertson, M. L., Chang, K. H., Gramlich, W. M., Hillmyer, M. A. *Macromolecules.* 2010, 43, 1807–1814.
32. Tang, Z. B., Zhang, C. Z., Liu, X. Q., Zhu, J. J. *Appl. Polym. Sci.* 2012, 125, 1108–1115.
33. Xing, Q., Zhang, X. Q., Dong, X., Liu, G. M., Wang, D. J. *Polymer.* 2012, 53, 2306–2314.
34. Yew, G. H., MohdYusof, A. M., MohdIshak, Z. A., Ishiaku, U.S. *Polym. Degrad. Stab.* 2005, 90, 488-500.
35. Shogren, R. L., Swanson, C. L., Thompson, A. R. *Starch.* 1992, 44, 335–338.
36. Lourdin, D., Coignard, L., Bizot H., Colonna, P. *Polymer.* 1997, 38, 5401-5406.
37. Forssell, P., Mikkila, J. M., Moates, G. K., Parker, R. *Carbohydr. Polym.* 1998, 34, 275–282.
38. Dai, X., Xiong, Z., Na, H., Zhu, J. *Compos. Sci. Technol.* 2014, 90, 9-15.

Received: 14-04-2017

Accepted: 26-05-2017